Am J Cancer Res 2022;12(10):4721-4736
www.ajcr.us /ISSN:2156-6976/ajcr0144142

Original Article

Deglycosylation of SLAMF7 in breast cancers enhances phagocytosis

Shih-Han Wang[1], Wen-Cheng Chou[1], Hsiang-Chi Huang[1], Te-An Lee[1], Tzu-Chun Hsiao[1], Ling-Hui Wang[1], Ke-Bin Huang[2], Chun-Tse Kuo[1], Chi-Hong Chao[3,4,5], Shing-Jyh Chang[6], Jung-Mao Hsu[7], Jialei Weng[8], Ning Ren[8,9], Fu-An Li[1], Yun-Ju Lai[10], Chenhao Zhou[8], Mien-Chie Hung[7,11], Chia-Wei Li[1]

[1]Institute of Biomedical Sciences, Academia Sinica, Taipei 115, Taiwan; [2]State Key Laboratory for Chemistry and Molecular Engineering of Medicinal Resources, School of Chemistry and Pharmacy, Guangxi Normal University, Guilin 541004, PR China; [3]Department of Biological Science and Technology, National Yang Ming Chiao Tung University, Hsinchu 30010, Taiwan; [4]Institute of Molecular Medicine and Bioengineering, National Yang Ming Chiao Tung University, Hsinchu 30010, Taiwan; [5]Center For Intelligent Drug Systems and Smart Bio-devices (IDS2B), National Yang Ming Chiao Tung University, Hsinchu 30010, Taiwan; [6]Hsinchu MacKay Memorial Hospital, Hsinchu, Taiwan; [7]Graduate Institute of Biomedical Sciences, Research Center for Cancer Biology and Center for Molecular Medicine, China Medical University, Taichung, Taiwan; [8]Department of Liver Surgery, Liver Cancer Institute, Zhongshan Hospital, and Key Laboratory of Carcinogenesis and Cancer Invasion (Ministry of Education), Fudan University, Shanghai, PR China; [9]Institute of Fudan Minhang Academic Health System (AHS), and Key Laboratory of Whole-period Monitoring and Precise Intervention of Digestive Cancer (SMHC), Minhang Hospital & AHS, Fudan University, Shanghai, PR China; [10]Solomont School of Nursing, Zuckerberg College of Health Sciences, University of Massachusetts Lowell, Lowell, MA, USA; [11]Department of Biotechnology, Asia University, Taichung, Taiwan

Received May 14, 2022; Accepted August 28, 2022; Epub October 15, 2022; Published October 30, 2022

Abstract: N-linked glycosylation of proteins is one of the post-translational modifications (PTMs) that shield tumor antigens from immune attack. Signaling lymphocytic activation molecule family 7 (SLAMF7) suppresses cancer cell phagocytosis and is an ideal target under clinical development. PTM of SLAMF7, however, remains less understood. In this study, we investigated the role of N-glycans on SLAMF7 in breast cancer progression. We identified seven N-linked glycosylation motifs on SLAMF7, which are majorly occupied by complex structures. Evolutionally conserved N98 residue is enriched with high mannose and sialylated glycans. Hyperglycosylated SLAMF7 was associated with STT3A expression in breast cancer cells. Inhibition of STT3A by a small molecule inhibitor, N-linked glycosylation inhibitor-1 (NGI-1), reduced glycosylation of SLAMF7, resulting in enhancing antibody affinity and phagocytosis. To provide an on-target effect, we developed an antibody-drug conjugate (ADC) by coupling the anti-SLAMF7 antibody with NGI-1. Deglycosylation of SLAMF7 increases antibody recognition and promotes macrophage engulfment of breast cancer cells. Our work suggests deglycosylation by ADC is a potential strategy to enhance the response of immunotherapeutic agents.

Keywords: SLAMF7, STT3A, breast cancer, deglycosylation, antibody-conjugate drug (ADC), NGI-1

Introduction

The complex interactions between innate and adaptive immune cells result in the antitumor immune response [1]. Modern research investigated cancers could secrete innate immune checkpoint inhibitors known as “don’t eat me signal” to avoid phagocytosis by macrophages and NK cells [1-3]. Blocking such “don’t eat me” signals, including CD47, CD24, and CD22 could be an effective treatment for various malignancies [1, 4-6]. In addition, discovering other “don’t eat me” signals could be another valuable foundation for eliminating tumors.

The self-ligand receptors of the signaling lymphocytic activation molecule family (SLAMF) receptors are cell surface glycoproteins on immune cells that participates phagocytosis [7]. As one of the SLAMF members, SLAMF7,

also called CD319 [8, 9], expresses on plasma cells [10], myeloma cells [11], and immune cells, such as natural killer (NK) cells [9, 12, 13], T cells [14, 15], macrophages, and monocytes [16]. SLAMF7 has the unique binding property to another SLAMF7 as a self-ligand through the amino-terminal Ig-like variable extracellular domain [17]. It possesses both activating and inhibitory functions in NK cells [9, 18]. In B lymphocytes, SLAMF7 induces the proliferation and production of autocrine cytokines [19]. During the bacterial infection, it suppresses pro-inflammatory cytokine production in LPS-activated monocytes [20]. SLAMF7 is also an essential molecule for the interaction between immune cells and cancer cells [21]. It acts as a positive regulator for NK cell activation by binding to Ewing's sarcoma-associated transcript 2 (EAT-2) in multiple myeloma (MM) [13]. Elotuzumab, an antibody targeting SLAMF7, enhances NK cells triggered antibody-dependent cellular cytotoxicity (ADCC) of myeloma cells and has been approved for clinical use [12, 13, 22-24]. Even though monoclonal antibody therapy has been developed [25-27], a poor response was found in patients with high soluble SLAMF7 levels in the serum [28]. As for the solid tumor, SLAMF7 can cause T cell exhaustion by inducing the expression of multiple inhibitory receptors [15]. Nevertheless, the function of SLAMF7 on other solid tumors has not been explored completely.

Breast cancer was the most frequent cancer globally, accounting for 12.5% of all new cases diagnosed in 2020. Triple-negative breast cancers (TNBCs) contribute 10-15% of all breast cancers, and these tumors are characterized by recurring malignancies associated with a poor prognosis, high ratio of metastasis, and a limited amount of treatment approaches [29]. Atezolizumab and pembrolizumab, two immune checkpoint inhibitors (ICI), were approved for patients with TNBC who express PD-L1 [30]. However, Atezolizumab was withdrawn from US FDA by Genetech on the TNBC indication due to the failure of the post-market clinical trial, IMpassion131, in 2021 [31]. It has been proposed that this might be caused by the inappropriate strategy to select breast cancer patients as a deglycosylation procedure seems to provide a better selection for patients to be treated with Atezolizumab. However, the data was from only nine patients, a small cohort that needs further validation with a larger cohort [31]. Glycosylated-PD-L1 on cancer cells also suppresses the activity of T cells [32]. Compared to normal cells, tumor cells exhibit widely divergent extracellular glycans due to abnormal glycosylation [33-36]. Glycan shield acts in multiple ways to escape from the immune system, including prevention of antibody recognition and suppression of T cell activity [32, 37-39]. It has been reported that N-glycans covered on tumor cells result in interfering cytotoxicity of chimeric antigen receptor (CAR)-engineered T cells [39]. Removing N-linked glycans from programmed death-ligand 1 (PD-L1) leads to enhanced PD-L1 antibody recognition [40]. Disrupting N-glycans synthesis by 2-deoxy-d-glucose (2-DG) also increases CAR T cell activity [39]. Evidence suggests that removing N-linked glycans from tumor antigens might be a promising approach to improve immunotherapy response.

N-linked glycosylation occurs in the endoplasmic reticulum (ER) lumen during post-translational modification, which plays a crucial role in maintaining the physiological function, such as enzyme activities, protein-protein interaction, and protein stability [41]. Oligosaccharyltransferase (OST) is a membrane-associated enzyme complex that catalyzes the N-linked glycosylation of protein in the ER lumen. It comprises two subunits, the STT oligosaccharyltransferase complex catalytic subunit A (STT3A) and the STT subunit B (STT3B). The previous study showed that STT3 could induce PD-L1 glycosylation to promote cancer stemness and immune evasion [42], reducing immunotherapy-targeted PD-1/PD-L1 [43]. STT3A is also required for spike glycosylation to determine viral infection [44] and induce breast cancer metastasis [45] upon SARS-CoV-2 infection. Altogether, aberrant protein glycosylation is critical in protein-protein and protein-antibody interaction contributing to disease progression.

Antibody-drug conjugates (ADCs) represent a new class of cancer therapeutics that deliver efficacious drugs to malignant cells. ADCs target specific tumor antigens, therefore avoiding off-target toxicity. The US Food and Drug Administration (FDA) has authorized 12 ADCs, including sacituzumab govitecan, an ADC of anti-Trop2 (trophoblast cell-surface antigen 2)

for TNBC in 2022, while more than 100 others are now being studied in clinical trials [46]. This study demonstrated that SLAMF7 is heavily N-linked glycosylated by STT3A in breast cancer cells. Deglycosylation of SLAMF7 by STT3A inhibitor may enhance the affinity of antibodies against SLAMF7. Our study provided an effective strategy to treat breast cancer through ADC by removing glycosylation on membrane proteins.

Results

SLAMF7 is an N-linked glycosylated protein

Glycosylation is an enzyme-directed site-specific process, where N-glycosylation generally occurs at the consensus motif (NXT/S) [41]. The evolutionarily conserved NXT motifs of SLAMF7 from different species were obtained from the National Center for Biotechnology Information (NCBI) to determine glycosylation sites [47]. Intriguingly, sequence alignment showed that SLAMF7 contains seven glycosylation consensus motifs (NXT/S) (N56, N98, N142, N148, N172, N176, and N204) which are located in the extracellular domain (ECD) (**Figure 1A** and **1B**). As shown in **Figure 1A**, the highly conserved motifs were found at N98, N142, and N148. The glycoforms of SLAMF7 were analyzed using a nanospray LC-MS/MS on a Tribrid Mass Spectrometer coupled to an Easy-nLC 1200 System. The numbers of peptide spectrum matches (PSM) revealed that the most abundant glycosylation sites were N56, N98, and N172, among these seven motifs (**Figure 1C**). The N-glycans at N98, N142, and N148 were majorly occupied by complex structures (**Figures 1C**, S1, S2). Based on LC-MS/MS identification, the N-glycans at N98 were occupied by high mannose and complex structures, including sialic acid-carrying glycans (**Figures 1D**, S1).

We further substituted the three asparagines (N) of those NXT/S glycosylation sites with glutamine (Q) (3NQ), with the molecular weight of SLAMF7 protein from SLAMF7 3NQ being lower than that of WT (**Figure 1E**). In addition, the molecular weight of SLAMF7 7NQ, which substituted all asparagines (N) of those NXT/S glycosylation sites with glutamine (Q), was around 39 kDa. We noticed that SLAMF7 protein expressed in HEK293 cells without PNGase F treatment has a ~15 kDa molecular weight shift up from their actual size (~39 kDa), indicating that SLAMF7 is modified with PTM. To further confirm whether SLAMF7 is modified with N-linked glycosylation, the Flag-tagged SLAMF7 was expressed in human HEK293 cells followed by various glycosylation inhibitor treatments for 24 hours. Interestingly, a reduced molecular weight of SLAMF7 was observed after applying N-linked glycosyltransferase inhibitors (**Figure 1F**, lanes 2-4) rather than O-GlcNAc-β-N-acetylglucosaminidase, O-GlcNAcase, and O-linked glycosyltransferase inhibitors (**Figure 1F**, lanes 5-9), indicating that SLAMF7 is highly modified by N-linked glycosylation. Furthermore, recombinant SLAMF7 only consisted of the extracellular domain and was treated with PNGase F or Endo H. Due to glycosylation, the apparent molecular mass of recombinant SLAMF7 is approximately 35-45 kDa in SDS-PAGE under reducing conditions. After treating PNGase F to remove both complex and hybrid N-linked glycans from polypeptides, the molecular weight was around 25 kDa, which was similar to predict molecular mass. The result confirmed that the SLAMF7 is extensively modified by the N-linked glycosylation (**Figure 1G**).

Expression of SLAMF7 in breast cancer cells

To investigate whether SLAMF7 plays an essential role in other solid tumors in addition to MM, the Genotype-Tissue Expression (GTEx) dataset and The Cancer Genome Atlas (TCGA) cancer dataset was used to investigate the relationship between SLAMF7 and solid tumors. Based on the normal tissue-derived GTEx dataset, SLAMF7 is conventionally expressed in various tissues, including spleen, colon, lung, and breast tissues (Figure S3A). According to the comparison of SLAMF7 expression between the male and female group, SLAMF7 in female breast tissue is most differentially upregulated as presented, revealing the pivotal role of SLAMF7 in the mammary tissue (Figure S3B). The SLAMF7 RNA expression was higher in breast tumors than in normal tissue in the TCGA breast cancer dataset (**Figure 2A**). Moreover, disease-free survival (DFS) for breast cancer patients from the Kaplan-Meier (KM) plotter dataset showed higher SLAMF7 expression is associated with a poor prognostic outcome (**Figure 2B**), which indicates that the SLAMF7 expression correlates with breast

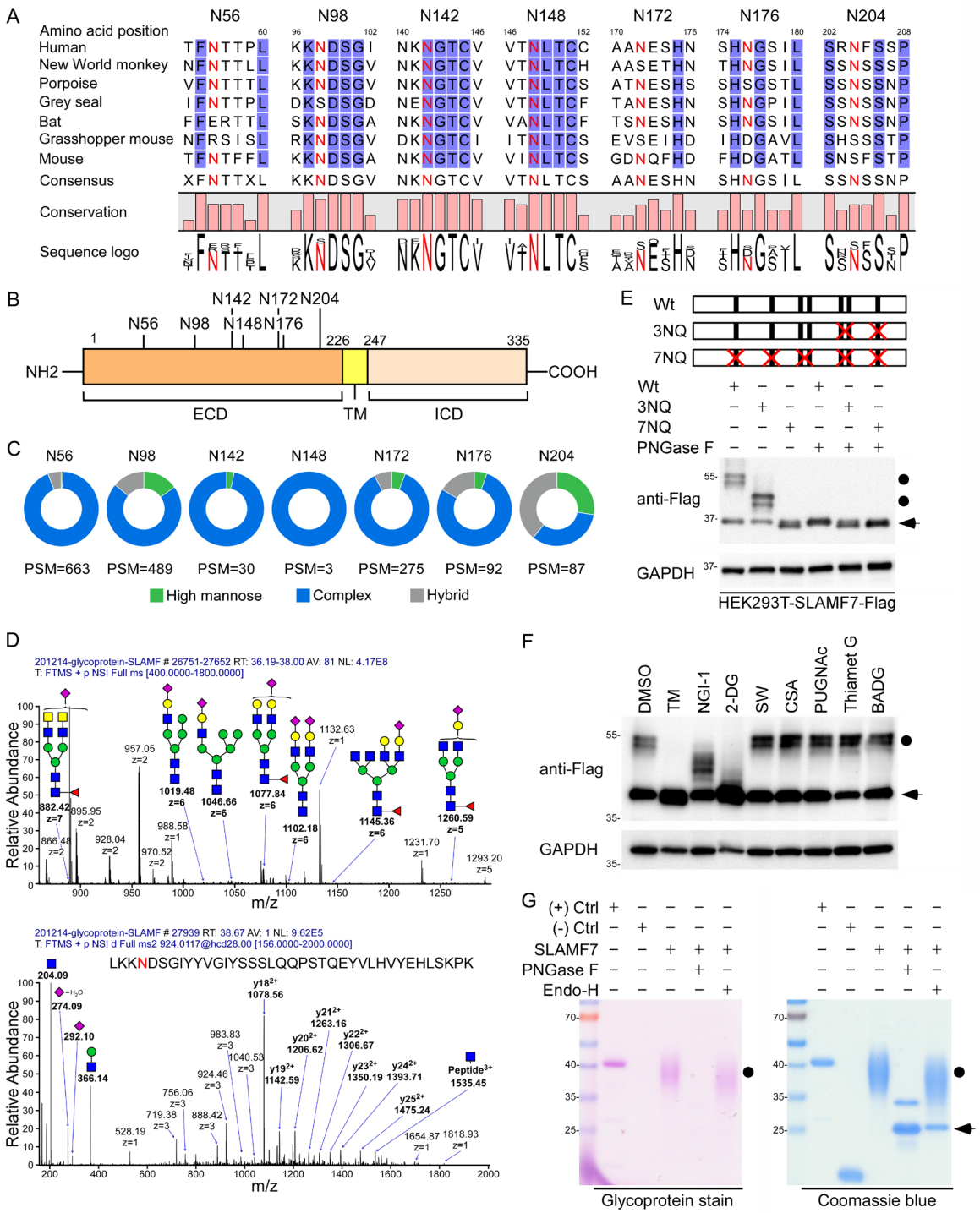

Figure 1. N-linked glycosylation of SLAMF7. A. Sequence alignment of SLAMF7 amino acid in seven species for evolutionarily conserved NXT/S motifs. N residues in NXT/S motifs are highlighted in red. B. Schematic diagram of SLAMF7 with seven N-link glycosylation sites. Full-length SLAMF7 was separated into the extracellular domain (ECD), transmembrane domain (TM), and intracellular domain (ICD). C. Distributions of the three types of N-glycans (high-mannose, hybrid, and complex) among SLAMF7 glycosylation sites were shown as pie charts. D. LC-MS/MS-based identification of N98 glycopeptides. The LC-MS profiles are shown as spectra averaged throughout elution time when a representative subset of glycoforms was detected. The cartoon symbols used for the glycans conform to the standard representation recommended by the Consortium for Functional Glycomics. E. Western blot analysis of wild type (Wt) and mutant (3NQ and 7NQ) SLAMF7 expression pattern in HEK293T cells. HEK293T cells were transfected with SLAMF-7 wild type, 3NQ, and 7NQ. After 48 h, protein samples were extracted from cells and treated with or without PNGase F. F. Western blot analysis of SLAMF7 expression pattern in HEK293T cells

treated with N-linked, O-GlcNAc-β-N-acetylglucosaminidase, O-GlcNAcase, or O-linked glycosyltransferase inhibitors. The non-glycosylated form in lane 2 represents SLAMF7 with Tunicamycin (TM) treatment overnight. N-linked inhibitors were included Tunicamycin (TM; 2.5 μg/mL), NGI-1 (10 μM), 2-DG (20 mg/mL), Swainsonine (SW; 10 μM), and Castanospermine (CSA, 50 μM). O-GlcNAc-β-N-acetylglucosaminidase inhibitor was PUGNAc (10 μM). O-GlcNAcase inhibitor was Thiamet G (10 μM). O-linked glycosyltransferase inhibitor was Benzyl 2-acetamido-2-deoxy-α-D-galactopyranoside (BADG, 10 μM). G. The glycosylation pattern of SLAMF7. Recombinant SLAMF7 protein with His tag at the C-terminus was treated with PNGase F or Endo H, and analyzed by glycoprotein staining (left panel). Coomassie blue staining on the right panel indicates the total amount of *SLAMF7* protein. Black circle, glycosylated SLAMF7; arrowhead, non-glycosylated SLAMF7.

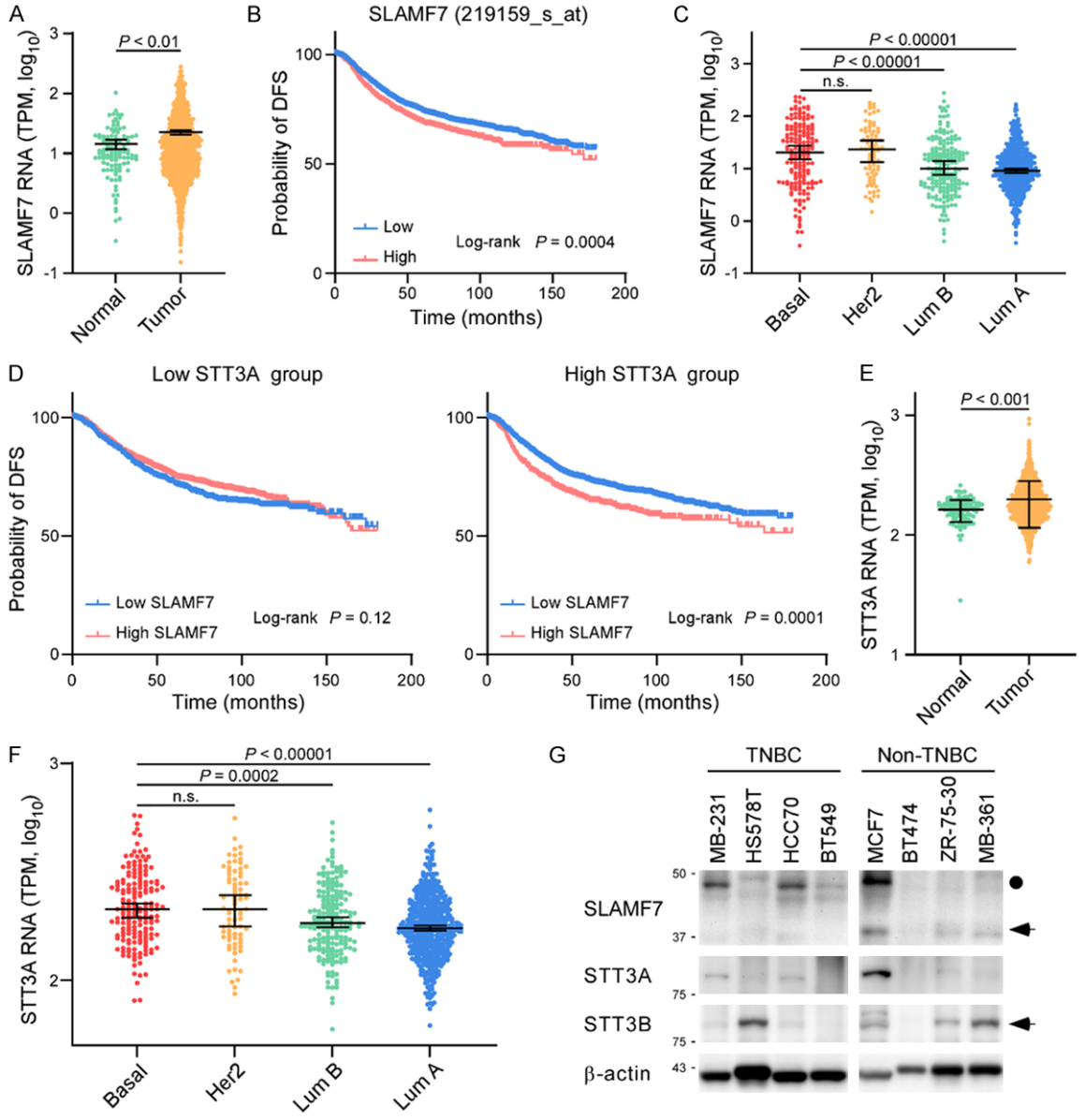

Figure 2. SLAMF7 expression profile in breast cancer. A. Analysis of SLAMF7 expression in TCGA normal breast or tumor tissues. *P*-values were calculated by *t*-test. B. Disease-free survival for breast cancer patients from KM plotter dataset. Patients were divided according to their SLAMF7 expression. *P*-values were calculated by the log-rank test. C. Differential expression of SLAMF7 in different breast cancer subtypes. *P*-values were calculated by one-way ANOVA. D. Disease-free survival (DFS) for breast cancer patients with below or above-median STT3A expression. Patients were divided according to their SLAMF7 expression. *P*-values were calculated by the log-rank test. E. Analysis of SLAMF7 expression in TCGA normal breast or tumor tissues. *P*-values were calculated by *t*-test. F. Differential expression of STT3A in different breast cancer subtypes. *P*-values were calculated by one-way ANOVA. G. Western blot of SLAMF7, STT3A, and STT3B protein expression in various breast cancer cell lines. Black circle, glycosylated SLAMF7; arrowhead, non-glycosylated SLAMF7.

tumor incidence. According to the TCGA breast cancer dataset, the SLAMF7 expression in the basal and Her2 types of breast cancer cells was higher than in luminal A and luminal B types (**Figure 2C**). Previous results showed that glycosites on SLAMF7 are majorly occupied by N-glycans (**Figure 1D**). In mammals, STT3A mediates co-translational N-linked glycosylation of nascent polypeptides, while STT3B is necessary for effective co-translational and post-translational glycosylation of secreted protein [48]. Disease-free survival (DFS) for breast cancer patients with below or above-median STT3A expression revealed that higher STT3A accompanied by higher SLAMF7 expression had a lower survival rate (**Figure 2D**). Thus, the association between SLAMF7 expression and DFS of breast cancers can be adjusted by the STT3A level. In the TCGA breast cancer dataset, breast cancer patients are prone to higher STT3A expression than normal people (**Figure 2E**). Furthermore, STT3A expression in basal and Her2 types of breast cancer is also higher than the other two types (**Figure 2F**), implying a positive correlation between STT3A expression and breast cancers. Western blot analysis revealed that glycosylated SLAMF7 expression was more abundant in MDA-MB-231, HCC70, and MCF-7, with higher STT3A expression (**Figure 2G**). Taken together, we postulated that the expression of SLAMF7 in breast cancer is associated with STT3A.

Deglycosylation of SLAMF7 through inhibiting STT3A by NGI-1

To demonstrate if STT3 isoforms play a role in SLAMF7 glycosylation in MDA-MB-231 cells, we used STT3 inhibitor and shRNA to downregulate STT3 activity and expression, respectively. Western blotting analysis revealed that decreasing STT3A activity by NGI-1, a small-molecule inhibitor of STT3, suppressed the SLAMF7 glycosylation dose-dependent (**Figure 3A**). Furthermore, knocking down STT3A decreased SLAMF7 glycosylation, as a significantly lower molecular weight of SLAMF7 was observed in STT3A-KD cells (**Figure 3B**), suggesting that STT3A catalyzes the N-glycosylation of SLAMF7.

N-linked glycosylation plays an essential role in regulating protein structure, stability, and function [49]. For instance, the glycan structure regulates SARS-CoV-2 viral entry and functions on shielding recognition sites of antibodies [44]. Deglycosylation on SLAMF7 might reduce its “don’t eat me” signaling, enhancing macrophage-dependent phagocytosis. To investigate if glycosylation of SLAMF7 inhibits phagocytosis, we conducted time-lapse imaging to examine phagocytosis. MDA-MB-231 cells were pre-treated with NGI-1 and then co-cultured with THP-1 differentiated macrophages. Time lapsed imaging by high content microscopy showed that NGI-1 treatment increases THP-1 macrophage-mediated phagocytosis of MDA-MB-231 cells (**Figure 3C**). After quantification by MetaXpress system, THP-1 macrophages displayed increased phagocytosis toward NGI-1-treated MDA-MB-231 cells after 4 hours of co-culture (**Figure 3D**). Our results indicate that targeting STT3A might be a novel strategy to enhance macrophage-mediated tumor cell phagocytosis.

SLAMF7 antibody-drug conjugate enhances antibody affinity

In addition to targeting STT3A, the SLAMF7 blockade in breast cancer cells might enhance phagocytosis. To validate this hypothesis, MDA-MB-231 cells were pre-incubated with IgG or anti-SLAMF7 antibody for 1 hour and then co-cultured with THP-1 macrophages. As shown in **Figure 4A**, anti-SLAMF7-treatment slightly enhanced phagocytosis compared to IgG-treatment. This slight engulfment induced by anti-SLAMF7 might be because of glycans on SLAMF7 shield antibody recognition. Indeed, removing the glycans on SLAMF7 by PNGase F treatment enhances anti-SLAMF7 affinity (**Figure 4B**). To provide on-target deglycosylation, we developed an ADC by crossing linking anti-SLAMF7 antibody with NGI-1 (SLAMF7-ADC) using a cleavable linker (MC-Val-Cit-PAB-OH), which was confirmed by direct-infusion MS analysis (**Figure 4C**). Flow cytometry analysis revealed that SLAMF7-ADC had a higher binding affinity to MDA-MB-231 cells than SLAMF7 antibody or IgG (**Figure 4D**). We then examined the effect of SLAMF7-ADC on modulating phagocytosis by flow cytometry (**Figure 4E**). Breast cancer cells stained with DAPI were pre-treated with IgG, anti-SLAMF7 antibody or SLAMF7-ADC and then co-cultured with THP-1 derived macrophages, which were pre-stained with 1 μM carboxyfluorescein succinimidyl ester (CFSE). Phagocytosis is shown as the per-

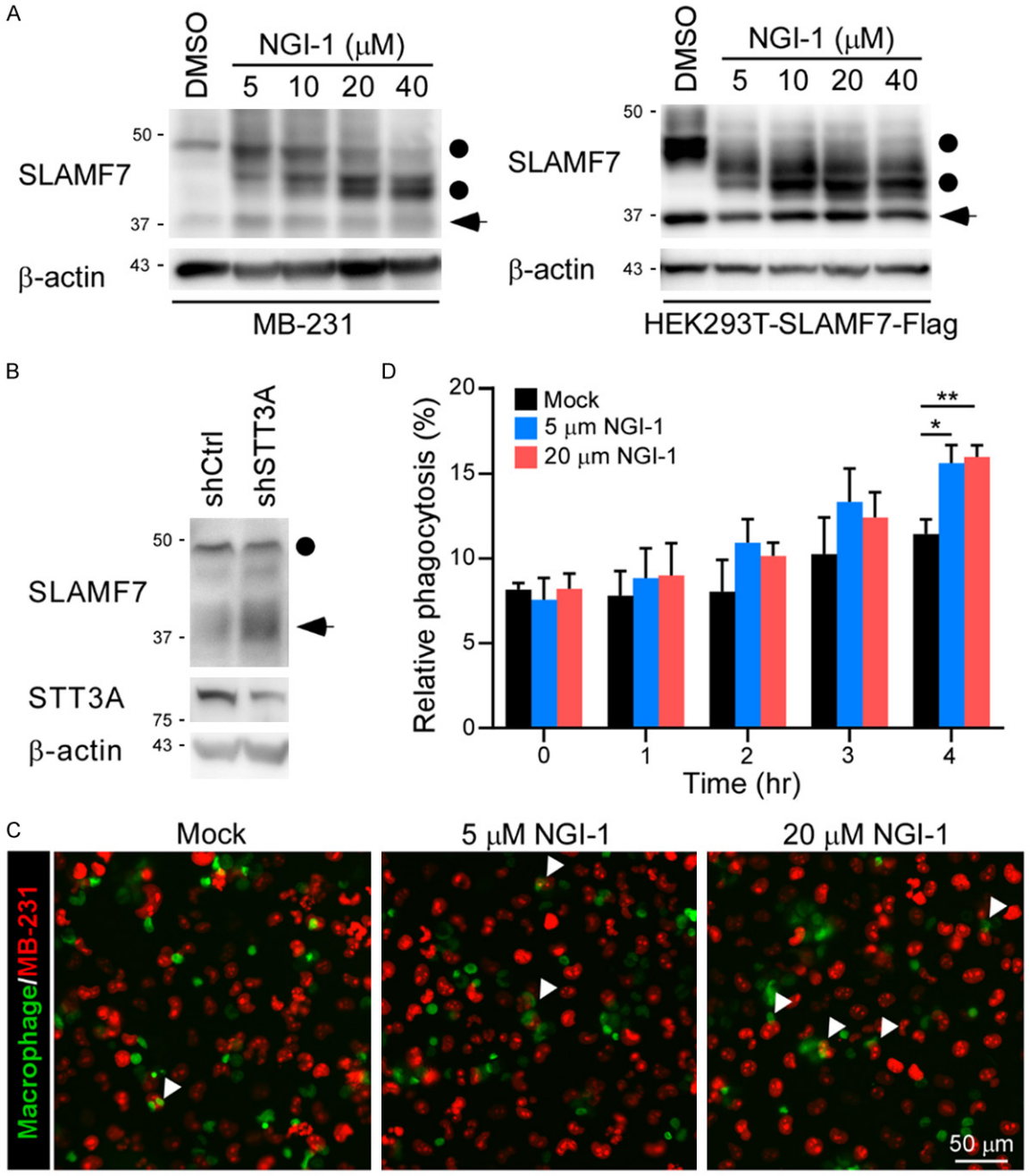

Figure 3. Inhibition of STT3A in breast cancer cells enhances phagocytosis. (A) The SLAMF7 protein expression of SLAMF7 in MDA-MB-231 cells and HEK293T-SLAMF7 cells. Cells were treated with various concentrations of NGI-1 as indicated. (B) Western blotting of SLAMF7, STT3A, and β-actin expression in MDA-MB-231 cells. STT3A expression was knocked down through lentiviral short-hairpin RNA (shRNA) in MDA-MB-231 cells. Beta-actin as an internal control. (C) Representative images of phagocytosis of tumor cells by THP-1 macrophages. MDA-MB-231 cells treated with various NGI-1 were incubated with THP-1 macrophages. MDA-MB-231 cells were labeled nucleus by red fluorescent protein (RFP). THP-1 macrophages were stained with DAPI. Arrows, individual phagocytosed MDA-MB-231 cells. The images were acquired by ImageXpress Micro Imaging XL System and (D) the quantitative analysis was performed by MetaXpress. *, $P<0.05$; **, $P<0.01$. *P*-values were calculated by two-way ANOVA. Black circle, glycosylated SLAMF7; arrowhead, non-glycosylated SLAMF7.

centage of $CFSE^{+}CD11b^{+}$ phagocyted cancer cells. As shown in **Figure 4F**, the phagocytosis was significantly increased in SLAMF7-ADC treated group compared to the SLAMF7 group.

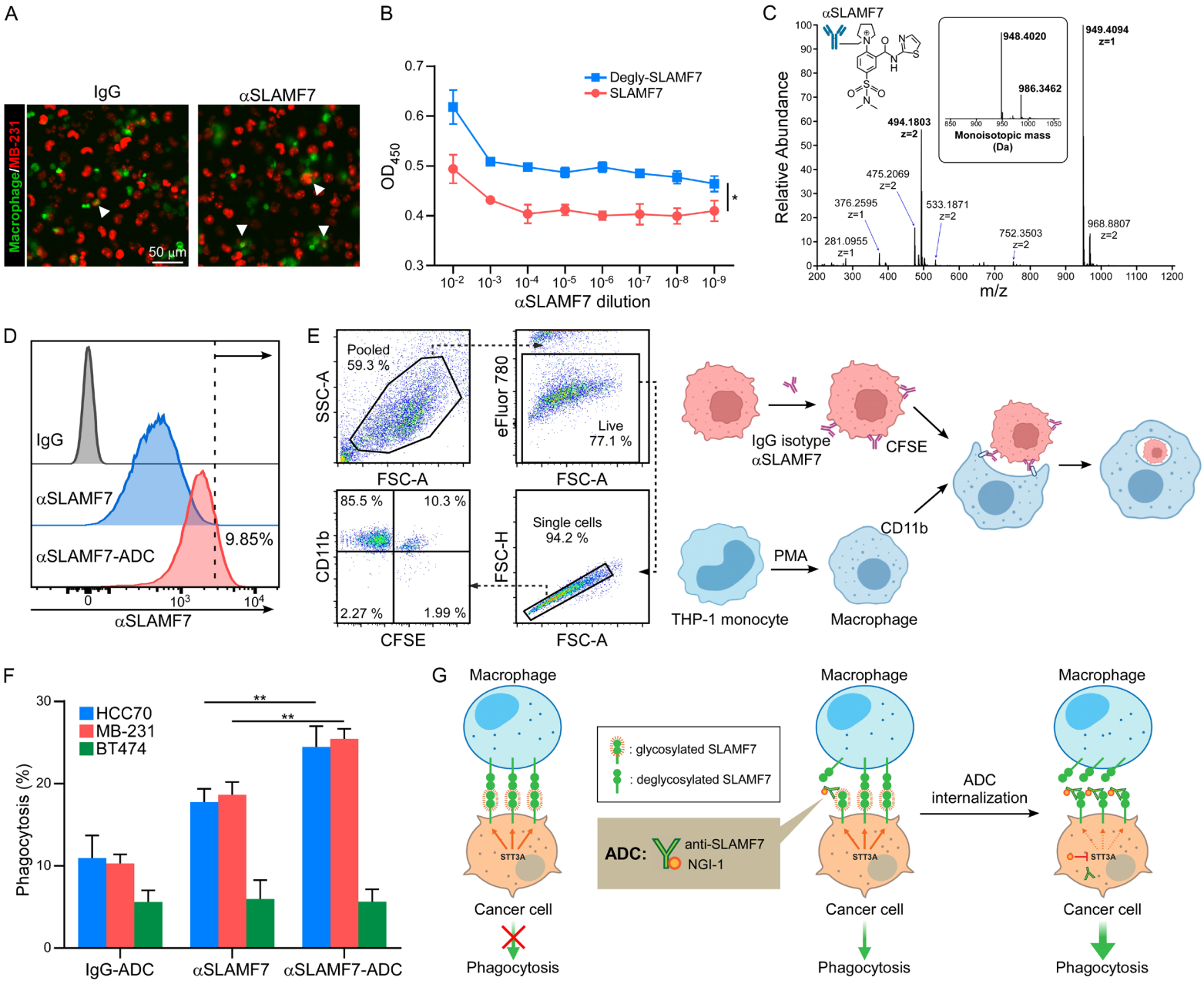
A
IgG
αSLAMF7
Macrophage/MB-231
50 μm
B
Degly-SLAMF7
SLAMF7
OD450
αSLAMF7 dilution
C
αSLAMF7
Relative Abundance
m/z
948.4020
949.4094 z=1
986.3462
494.1803 z=2
475.2069 z=2
376.2595 z=1
533.1871 z=2
752.3503 z=2
968.8807 z=2
281.0955 z=1
Monoisotopic mass (Da)
D
IgG
αSLAMF7
αSLAMF7-ADC
9.85%
αSLAMF7
E
Pooled 59.3 %
SSC-A
FSC-A
eFluor 780
Live 77.1 %
85.5 %
10.3 %
2.27 %
1.99 %
CD11b
CFSE
Single cells 94.2 %
FSC-H
IgG isotype
αSLAMF7
CFSE
CD11b
PMA
THP-1 monocyte
Macrophage
F
HCC70
MB-231
BT474
Phagocytosis (%)
IgG-ADC
αSLAMF7
αSLAMF7-ADC
G
Macrophage
: glycosylated SLAMF7
: deglycosylated SLAMF7
ADC:
anti-SLAMF7
NGI-1
STT3A
Cancer cell
Phagocytosis
ADC internalization

Figure 4. Enhancement of macrophage-mediated tumor cell phagocytosis by SLAMF7-ADC. A. High content image of THP-1 macrophages that phagocytosed MDA-MB-231 breast cancer cells. MDA-MB-231 cells carrying RFP in the nucleus were pre-treated with NGI-1 as indicated overnight and then co-cultured with THP-1 macrophages for 4 hours. Arrows, individual phagocytosed MDA-MB-231 cells. B. ELISA detection of the indicated diluted anti-SLAMF7 antibody binding to precoated SLAMF-7 after PNGase F treatment. Data shown are means ± SD from representative triplicates from three independent experiments. **, P<0.05. P-values were calculated by t-test.* C. Data deconvolution revealed a monoisotopic mass for the Linker+NGI-1 of 948.4020 Da. D. Flow cytometry analysis of IgG, anti-SLAMF7 antibody, and SLAMF7-ADC binding to MDA-MB-231. E. Flowchart of phagocytosis and Flow cytometry gating strategy. F. Phagocytosis of THP-1 macrophages co-cultured with antibody-treated breast cancer cells. HCC70, MDA-MB-231, and BT474 cells pre-treated with IgG, anti-SLAMF7 antibody, or SLAMF7-ADC were stained with CFSE and then co-cultured with THP-1 macrophages. Phagocytosis of THP-1 macrophages was determined by flow cytometry. **, *P*<0.01. *P*-values were calculated by two-way ANOVA. G. Illustration of glycosylation function of SLAMF7 in breast cancer. (i) SLAMF7 on breast cancer cells interacts with macrophages to avoid phagocytosis. (ii) SLAMF7-ADC targets and internalizes breast cancer cells. Next, NGI-1 released from ADC deglycosylates SLAMF7. Increased macrophage engulfment as a result of SLAMF7 signal blockage.

In addition, SLAMF7-ADC treated HCC70 and MDA-MB-231 cells had a higher phagocytic rate than BT474 cells, which had no expression of SLAMF7. These results indicated that SLAMF7-ADC could specifically inhibit N-glycosylation of SLAMF7 in breast cancer cells and enhance macrophage phagocytic activity (**Figure 4G**).

Discussion

The previous study showed that SLAMF7 expression on hematopoietic cancer cells is required for phagocytosis upon treatment with a CD47 blocking therapeutic antibody [50]. Depletion of SLAMF triggered macrophage phagocytosis of hematopoietic cells *in vitro* and *in vivo* [51]. However, recent research discovered that SLAMF7 expression in cancer cells is unnecessary for CD47-mediated phagocytosis [52]. To elucidate the impact of cancer-expressing SLAMF7 on phagocytosis, we disrupted the SLAMF7 glycosylation, which led to the promotion of macrophage-mediated phagocytosis. We suggested that rather than being required for CD47-mediated phagocytosis, SLAMF7 on solid tumors acts as a "don't eat me" signal to avoid phagocytosis.

Compared to non-malignant tissues, tumor cells exhibit different glycosylation patterns [33-36]. Increased understanding of the role of glycosylation on cancer-specific markers or microbe's components has led to the development of inhibitors or monoclonal antibodies to target the glycans. For instance, a glycosylation-specific PD-L1 antibody was designed to block the PD-1/PD-L1 axis and trigger PD-L1 degradation in lysosomes [53]. To date, treatment of solid tumors or hematologic malignancies by targeting glycosylation is under clinical investigation. In a phase 1/2 clinical trial, acute myeloid leukemia (AML) patients display a good prognosis and high remission rate after Uproleselan (GMI-1271) and E-selectin antagonist administration [54]. Galectin inhibitor GR-MD-02 is used to fight against various solid tumors, including head and neck squamous cell carcinoma, non-small cell lung cancer, and metastatic melanoma, along with immunotherapy in several phase 1 clinical trials [55]. In addition to reducing cancer malignancy, the ablation of glycosylation of viral proteins by glycosylation inhibitor or ADC reduces the infectivity of viruses such as SARS-CoV-2 [44, 56, 57], Ebola [58], and Lassa virus [59]. Although targeting glycosylation has been shown to exert therapeutic benefits toward diseases, global modulation of glycosylation might also lead to side effects since it plays a vital role in regulating multiple biological processes in diseased as well as normal cells. To avoid the off-target effects and increase the efficiency of therapeutics targeting glycosylation, a strategy that specifically targets disease-associated glycosylation is needed. Therefore, we developed a novel ADC to specifically reduce SLAMF7 glycosylation in cancer cells without affecting normal tissues. An inhibitor of oligosaccharyltransferases, NGI-1, inhibits N-linked glycosylation by impeding the transfer of lipid-linked oligosaccharides to recipient glycoproteins [60], was linked with anti-SLAMF7 monoclonal antibody (**Figure 4C**). This ADC can target and potentiate macrophage-induced phagocytosis toward SLAMF7-expressing cancer cells such as MDA-MB-231 and HCC70, but not BT474 cells that express only very low-level SLAMF7, suggesting a disease-specific inhibition on glycosylation (**Figure 4F**).

SLAMF7 has been studied extensively as a potential therapeutic target for MM [12, 13, 22-24, 61].

The monoclonal antibody therapy medication, Elotuzumab, targets SLAMF7 to induce macrophage activation and ADCC [25-27]. Additionally, other potential strategies have been developed to target SLAMF7, including bispecific antibody, ADC, and CAR T cell therapy [61, 62]. A method combining adoptive T-cell therapy with bispecific antibodies has been developed to target and treat solid and hematologic malignancies [63]. The bispecific anti-SLAMF7 × anti-CD3 antibody-armed activated T cells increase cytotoxicity and T cell expansion against MM cells [61]. It is worth noting that the first SLAMF7-ADC (ABBV-838) using cytotoxic MMAE as the payload shows limited efficacy in relapsed and refractory multiple myeloma patients [64], and high serum levels of soluble SLAMF7 in MM patients are accompanied by a worse response to Elotuzumab and shorter survival [28]. These studies suggest that increased soluble SLAMF7 can act as a decoy to neutralize immune-targeted agents and impair the therapeutic responses [65]. Although there is no evidence comparing the soluble SLAMF7 level in the serum of normal people and breast cancer patients, however, via the conjugation with NGI-1, our ADC exhibited a higher affinity toward SLAMF7 than the monoclonal antibody (**Figure 4D**), which might overcome the decoy ability of SLAMF7 in the serum. Taken together, our results showed that antibodies conjugating with glycosyltransferase inhibitors could increase antigen-binding affinity and thereby enhance the function of effector cells. Applying this strategy to other immunotherapeutics might have the potential to exert better clinical responses, which is in urgent need of investigation in the near future.

Materials and methods

Amino acid sequence alignment and homology analysis

Seven full-length amino acid sequences of SLAMF7 proteins were downloaded from the NCBI GenBank Database, including human (*Homo sapiens,* NP_067004.3), New World monkey (*Callithrix jacchus*, XP_002760223.2), porpoise (*Phocoena sinus*, XP_032464724.1), grey seal (*Halichoerus grypus*, XP_035940618.1), bat (*Pipistrellus kuhlii*, XP_036298484.1), southern grasshopper mouse (*Onychomys torridus*, XP_036058984.1), and mouse (*Mus musculus*, NP_653122.2). Seven NXT/S motifs in SLAMF7 were conducted and analyzed by QIAGEN CLC main workbench 20.0.4 (https://digitalinsights.qiagen.com).

Cell culture and transfection

HEK293T, MDA-MB-231, HS578T, HCC70, BT549, MCF-7, BT474, ZR-75-30, MDA-MB-361, and THP-1 cells were obtained from American Type Culture Collection (ATCC). HEK293T, MDA-MB-231, HS578T, MCF-7, and MDA-MB-361 cells were grown in DMEM/F12 medium supplemented with 10% fetal bovine serum (FBS). HCC70, BT549, BT474, ZR-75-30, and THP-1 cells were grown in RPMI 1640 medium supplemented with 10% fetal bovine serum (FBS). According to the user instruction, cells were transiently transfected with plasmids using X-tremeGENE HP DNA Transfection Reagent (Roche, Mannheim, Germany) for transient transfection.

Plasmids, antibodies, and chemicals

The pCMV3-SLAMF7-Flag construct (HG11691-CF) was purchased from Sino Biological (Beijing, China) to establish SLAMF7-Flag expression cell lines. Using the pCMV3-SLAMF7-Flag construct as a template, Biomedical Resource Core of the First Core Laboratory (National Taiwan University, Taipei, Taiwan) made SLAMF7-Flag NQ mutants [3NQ (N172Q, N176Q, and N204Q) and 7NQ (N56Q, N98Q, N142Q, N148Q, N172Q, N176Q, and N204Q)]. The following antibodies were used: Flag (F3165; Sigma-Aldrich, St. Louis, MO, USA), SLAMF7 (ab230945; Abcam, Cambridge, UK), GAPDH (60004-1-Ig; Proteintech, Chicago, IL, USA), STT3A (12034-1-AP; Proteintech), β-actin (110564; GeneTex, Irvine, CA, USA), Anti-Human/Mouse CD11b APC-Cy7 (25-0112-U025; Tonbo Biosciences, San Diego, CA, USA). Recombinant SLAMF7 protein (11691-H08H) was purchased from SinoBiological (Beijing, China). The following chemicals were used: Tunicamycin (TM) (T7765), NGI-1 (SML1620), 2-deoxy-glucose (2-DG) (D8375), Thiamet G (SML0244), Benzyl 2-acetamido-2-deoxy-α-D-galactopyranoside (BADG) (B4894), polybrene (H9268), and 3,3',5,5'-Tetramethylbenzidine (TMB) (T0440) were purchased from Sigma-

Aldrich (St. Louis, MO, USA); Swainsonine (SW) (16860), Castanospermine (CSA) (11313), and O-GlcNAc-β-N-acetylglucosaminidase inhibitor (PUGNAc) (17151) were purchased from Cayman Chemical Company (Ann Arbor, MI, USA); PNGase F (P0704L) and Endonuclease H (Endo H; P0702S) were purchased from New England Biolabs (Ipswich, MA, USA). EDTA-free protease inhibitor cocktail (4693132001) was purchased from Merck (Darmstadt, Germany). Puromycin (ant-pr-5) was purchased from InvivoGen (Occitanie, France).

Generation of stable cells using lentiviral infection

To establish a shSTT3A knockdown breast cancer cell line, the pLKO.1-based lentivirus shRNA vectors for STT3A (TRCN0000153679) and STT3B (TRCN0000139967) were obtained from the National RNAi Core Facility in Academia Sinica. The breast cancer cell line, MDA-MB-231, was infected with shSTT3A lentivirus and 10 μg/mL polybrene and then centrifuged at 800 × *g* for 2 hours. The medium was refreshed after 48 hours of viral transduction, and then the infected cells were subsequently selected with 1 μg/mL puromycin for a week. The pLKO.1-based lentivirus shRNA vector (TRC1 Scramble) was also transduced into MDA-MB-231 as the control group.

Western blotting

The cell culture dish was placed on ice, and the cells were washed with cold PBS. After lysing cells with RIPA buffer (150 mM NaCl, 0.1% sodium dodecyl sulfate, 1% sodium deoxycholate, 1% NP-40, 1 mM EDTA, protease inhibitors, and 50 mM Tris-HCl, pH 7.6), the protein concentration was quantified by Bradford assay (Bio-Rad, Hercules, CA, USA). Western Blotting analysis was performed as described previously [66]. Image acquisition was performed by UVP ChemStudio PLUS Touch imaging system (Analytik Jena AG, Jena, Germany).

Glycoprotein and Coomassie blue staining

The deglycosylation protocol was performed according to Huang et al. studies [44, 45]. After SLAMF7 protein was treated with PNGase F or Endo H for 3 hours, the proteins were then analyzed by SDS-PAGE. Total protein was stained with Bio-Safe™ Coomassie Stain (1610786; Bio-Rad). The glycoprotein was stained using Pierce™ Glycoprotein Staining Kit (24562; Thermo Fisher Scientific, Waltham, MA, USA). Horseradish peroxidase was used as a positive control, while soybean trypsin inhibitor was a negative control.

Identification of the N-glycopeptides

The procedure for N-glycopeptide identification was performed according to Huang et al. study [44]. Before LC-MS/MS analysis, the digested products were diluted with formic acid and cleaned up using ZipTip C18 (Millipore). The peptide mixture was analyzed by nanospray LC-MS/MS on a Tribrid Mass Spectrometer (Orbitrap Fusion Lumos, Thermo Fisher Scientific) coupled to an Easy-nLC 1200 System (Thermo Fisher Scientific). The MS raw data were searched for glycopeptide identification by using Byonic algorithm (v2.16.11) and the pGlyco algorithm (v3.0). The N-glycan database was searched against the database of 182 human with no multiple fucose glycan compositions and a score cutoff of 300. The glycan structure was drawn using GycoWorkbench.

Analysis of data from public datasets

The transcripts per million (TPM) normalized RNA sequences data for gene expression in various normal samples were retrieved from GTEx Analysis V8 (www.gtexportal.org). Gene expression for SLAMF7 and STT3A in breast cancer tissues were downloaded from the TCGA dataset. TPM-normalized gene expressions were used to calculate the differential expression and the results were plotted and tested for significance (t-test or One-Way ANOVA) using GraphPad Prism 9.20 (GraphPad). According to the KM Plotter website, relapse-free survival for patients with breast cancer was analyzed. According to the website instruction, all patients with breast cancer were split into two groups based on their expression of SLAMF7 only or combined with STT3A. The results were plotted and tested for significance (log-rank test) using GraphPad Prism.

Antibody-drug conjugate (ADC)

Conjugation of antibodies with NGI-1 was performed by using an MC-Val-Cit-PAB-OH linker according to the procedures of Huang et al. study [44]. Spectral analysis, residual thiol

group tests, and amino acid analyses were used to quantify protein and drug concentrations. Size-exclusion HPLC and C18 RP-HPLC were performed to ensure all conjugates >98% monomeric and <0.5% unconjugated cysteine quenched drug exists, respectively.

Identification of a MC-Val-Cit-PAB-OH linker with NGI-1 by direct-infusion MS

The samples of the MC-Val-Cit-PAB-OH linker with drug NGI-1 were dissolved in DMSO and diluted in 50% acetonitrile and 0.1% formic acid. The direct-infusion nESI (nano electrospray ionization) analysis was performed on an Orbitrap EliteTM mass spectrometer (Thermo Scientific). The mass spectrometer was operated in positive mode and nESI source was held at +2.4 kV. The Linker+NGI-1 was analyzed with the following acquisition parameters: the capillary temperature at 250°C; FT resolution set to 60,000 (at m/z 400); S-lens RF level at 20; scan range set at m/z 200-1,200; microscans set to 3; AGC target at 1×10^6; maximum injection time of 50 ms; averaging set at 10. Mass spectrometric raw data were deconvoluted using Xtract algorithm within Xcalibur 3.0 (Thermo Fisher Scientific).

Phagocytosis

Cultured THP-1 cells were induced to differentiate into phagocytic macrophages using PMA (200 nM). After 3 days of induction, THP-1 cells changed morphology and adhered to the culture dish. MDA-MB-231 cells were treated with NGI-1 for 24 hours or antibodies for 1 hour. To assay THP-1 macrophage phagocytosis, THP-1 macrophages were incubated in a serum-free medium for 2 hours before adding breast cancer cells. The live-cell images were acquired by the ImageXpress Micro Imaging XL System at 37°C with 5% CO_2. THP-1 macrophage was pre-stained by DAPI for live-cell images before being co-cultured with MDA-MB-231 cells, which had nuclear RFP. The phagocytic rate was quantified by using MetaXpress system. For flow cytometry, cancer cells were probed with antibodies at 37°C for 1 hour and incubated with 1 μM 5,6-carboxyfluorescein diacetate succinimidyl ester (CFSE) for 15 min. THP-1 macrophage were mixed with CFSE-labelled cancer cells in a ratio of 1:1 (total 2×10^5 cells) at 37°C for 2 hours. After washing two times with FACS buffer, the cell mixture was stained with CD11b-APC and viability dye eFluor™ 780. Flow cytometry analyzed the sample for phagocytosed CSFE-labelled cancer cells ($CFSE^+$ $CD11b^+$).

Enzyme-linked immunosorbent assay (ELISA)

SLAMF7 protein was coated on an ELISA plate followed by deglycosylation using PNGase F at 4°C overnight. After 2 hours of blocking with 3% BSA in PBS at room temperature (RT), a serially diluted anti-SLAMF7 antibody was added and incubated at RT for 2 hours. Both non-glycosylated and deglycosylated SLAMF7 were captured by antibody, and the non-captured antibody was removed by washing with PBS containing 0.05% Tween 20 (PBST) three times. Captured antibody was then treated with HRP-conjugated anti-mouse IgG (1:5000) at RT for 1 hour. After three times washing with PBST, the color reaction was developed by TMB and halted by the addition of HCl. The absorbance is measured at 450 nm by an ELISA reader, VERSAmax (Molecular Devices, San Jose, CA, USA).

Fluorescence-activated cell sorting (FACS) binding assay

MDA-MB-231 cells were analyzed for antibody binding affinity on a flow cytometer (AttuneTM NxT Flow Cytometer, Thermo Fisher Scientific). The cells were stained with SLAMF7 primary antibody, anti-rabbit IgG 488 secondary antibody, and viability dye eFluor™ 780. The negative control was the isotype IgG group. A total of 10,000 events were collected for each sample.

Statistical analysis

Data from individual experiments are presented as mean ± SD (standard deviation) and assessed by Mann-Whitney test, one-way, or two-way ANOVA with Tukey's post hoc test for multiple comparisons (GraphPad Prism Software Inc., San Diego, CA, USA). The relationships between SLAMF7 with STT3A in the TCGA cancer dataset retrieved from the TCGA database were analyzed by Pearson correlation analysis. A P value <0.05 was considered statistically significant.

Acknowledgements

This work was funded in part by the following: Ministry of Science and Technology (MOST

109-2314-B-001-002-MY3 and MOST 109-2314-B-001-008-MY3 to C.-W.L.; MOST 109-2628-B-009-004 to C.-H.C.; MOST 109-2327-B-039-003 and MOST 110-2639-B-039-001-ASP to M.-C.H.), Academia Sinica (AS-KPQ-111-KNT and AS-GC-110-05 to C.-W.L.), Higher Education Sprout Project by the Ministry of Education of Taiwan and the Cancer Prevention & Research Institutes of Texas (RP160710-P2 to M.-C.H.), Cancer Center support grant (NCI NIH P30 CA016672 to M.-C.H.), National Institutes of Health (5R01 AI116722 to M.-C.H.), Breast Cancer Research Foundation (BCRF 20-070 to M.-C.H.), National Natural Science Foundation of China (82103521 to C.Z.), the Shanghai Sailing Program (21YF1407500 to C.Z.), China Postdoctoral Science Foundation (2021M690674 to C.Z.), and University of Massachusetts Lowell (Faculty start-up D50-210000000022 to Y.-J.L.). The "Smart Platform of Dynamic Systems Biology for Therapeutic Development" and "Center for Intelligent Drug Systems and Smart Bio-devices (IDS2B) from The Featured Areas Research Center Program" within the framework of the Higher Education Sprout Project of the Ministry of Education (MOE) in Taiwan. Additionally, we thank the National RNAi Core Facility of Academia Sinica for the production of shRNA. We thank the Biomedical Resource Core of the First Core Laboratory at College of Medicine of National Taiwan University for the production of SLAFM7-3NQ and SLAMF7-7NQ plasmids. We also thank the Proteomic Core Facility, DNA Sequencing Core Facility (AS-CFII-108-115), Flow Cytometry Core Facility, and Light Microscopy Core Facility at the Institute of Biomedical Sciences of Academia Sinica for assistance in N-glycopeptide identification, DNA sequencing, analysis of flow cytometry, and morphological studies.

Disclosure of conflict of interest

H.-C.H. and C.-W.L. are inventors listed on patent applications in the filing.

Address correspondence to: Chenhao Zhou, Department of Liver Surgery, Liver Cancer Institute, Zhongshan Hospital, and Key Laboratory of Carcinogenesis and Cancer Invasion (Ministry of Education), Fudan University, Shanghai, PR China. E-mail: zhouchenhao@fudan.edu.cn; Mien-Chie Hung, Graduate Institute of Biomedical Sciences, Research Center for Cancer Biology and Center for Molecular Medicine, China Medical University, Taichung, Taiwan. E-mail: mhung@cmu.edu.tw; Chia-Wei Li, Institute of Biomedical Sciences, Academia Sinica, Taipei 115, Taiwan. E-mail: cwli@ibms.sinica.edu.tw

References

[1] Lentz RW, Colton MD, Mitra SS and Messersmith WA. Innate immune checkpoint inhibitors: the next breakthrough in medical oncology? Mol Cancer Ther 2021; 20: 961-974.

[2] Barkal AA, Brewer RE, Markovic M, Kowarsky M, Barkal SA, Zaro BW, Krishnan V, Hatakeyama J, Dorigo O, Barkal LJ and Weissman IL. CD24 signalling through macrophage Siglec-10 is a target for cancer immunotherapy. Nature 2019; 572: 392-396.

[3] Logtenberg MEW, Scheeren FA and Schumacher TN. The CD47-SIRPα immune checkpoint. Immunity 2020; 52: 742-752.

[4] Russ A, Hua AB, Montfort WR, Rahman B, Riaz IB, Khalid MU, Carew JS, Nawrocki ST, Persky D and Anwer F. Blocking "don't eat me" signal of CD47-SIRPα in hematological malignancies, an in-depth review. Blood Rev 2018; 32: 480-489.

[5] Takimoto CH, Chao MP, Gibbs C, McCamish MA, Liu J, Chen JY, Majeti R and Weissman IL. The macrophage 'Do not eat me' signal, CD47, is a clinically validated cancer immunotherapy target. Ann Oncol 2019; 30: 486-489.

[6] Pluvinage JV, Haney MS, Smith BAH, Sun J, Iram T, Bonanno L, Li L, Lee DP, Morgens DW, Yang AC, Shuken SR, Gate D, Scott M, Khatri P, Luo J, Bertozzi CR, Bassik MC and Wyss-Coray T. CD22 blockade restores homeostatic microglial phagocytosis in ageing brains. Nature 2019; 568: 187-192.

[7] van Driel BJ, Liao G, Engel P and Terhorst C. Responses to microbial challenges by SLAMF receptors. Front Immunol 2016; 7: 4.

[8] Sriram H, Ghogale S, Subramanian P, Yajamanam B, Deshpande N, Chatterjee G, Patkar N, Verma S, Jain H and Bagal B. Evaluation of CD319 (SLAMF7) as a novel gating marker for plasma cells in flow cytometric immunophenotyping of multiple myeloma. Clin Lymphoma Myeloma 2019; 19: e153.

[9] Tassi I and Colonna M. The cytotoxicity receptor CRACC (CS-1) recruits EAT-2 and activates the PI3K and phospholipase Cgamma signaling pathways in human NK cells. J Immunol 2005; 175: 7996-8002.

[10] Soh KT, Tario JD Jr, Hahn T, Hillengass J, McCarthy PL and Wallace PK. CD319 (SLAMF7) an alternative marker for detecting plasma

cells in the presence of daratumumab or elotuzumab. Cytometry B Clin Cytom 2021; 100: 497-508.
[11] Malaer JD and Mathew PA. CS1 (SLAMF7, CD319) is an effective immunotherapeutic target for multiple myeloma. Am J Cancer Res 2017; 7: 1637-1641.
[12] Pazina T, James AM, Colby KB, Yang Y, Gale A, Jhatakia A, Kearney AY, Graziano RF, Bezman NA, Robbins MD, Cohen AD and Campbell KS. Enhanced SLAMF7 homotypic interactions by elotuzumab improves nk cell killing of multiple myeloma. Cancer Immunol Res 2019; 7: 1633-1646.
[13] Campbell KS, Cohen AD and Pazina T. Mechanisms of NK cell activation and clinical activity of the therapeutic SLAMF7 antibody, elotuzumab in multiple myeloma. Front Immunol 2018; 9: 2551.
[14] Awwad MHS, Mahmoud A, Bruns H, Echchannaoui H, Kriegsmann K, Lutz R, Raab MS, Bertsch U, Munder M, Jauch A, Weisel K, Maier B, Weinhold N, Salwender HJ, Eckstein V, Hänel M, Fenk R, Dürig J, Brors B, Benner A, Müller-Tidow C, Goldschmidt H and Hundemer M. Selective elimination of immunosuppressive T cells in patients with multiple myeloma. Leukemia 2021; 35: 2602-2615.
[15] O'Connell P, Hyslop S, Blake MK, Godbehere S, Amalfitano A and Aldhamen YA. SLAMF7 signaling reprograms T cells toward exhaustion in the tumor microenvironment. J Immunol 2021; 206: 193-205.
[16] Maekawa T, Kato S, Kawamura T, Takada K, Sone T, Ogata H, Saito K, Izumi T, Nagao S, Takano K, Okada Y, Tachi N, Teramoto M, Horiuchi T, Hikota-Saga R, Endo-Umeda K, Uno S, Osawa Y, Kobayashi A, Kobayashi S, Sato K, Hashimoto M, Suzu S, Usuki K, Morishita S, Araki M, Makishima M, Komatsu N and Kimura F. Increased SLAMF7(high) monocytes in myelofibrosis patients harboring JAK2V617F provide a therapeutic target of elotuzumab. Blood 2019; 134: 814-825.
[17] Pazina T, MacFarlane AW 4th, Bernabei L, Dulaimi E, Kotcher R, Yam C, Bezman NA, Robbins MD, Ross EA, Campbell KS and Cohen AD. Alterations of NK cell phenotype in the disease course of multiple myeloma. Cancers (Basel) 2021; 13: 226.
[18] Cruz-Munoz ME, Dong Z, Shi X, Zhang S and Veillette A. Influence of CRACC, a SLAM family receptor coupled to the adaptor EAT-2, on natural killer cell function. Nat Immunol 2009; 10: 297-305.
[19] Lee JK, Mathew SO, Vaidya SV, Kumaresan PR and Mathew PA. CS1 (CRACC, CD319) induces proliferation and autocrine cytokine expression on human B lymphocytes. J Immunol 2007; 179: 4672-4678.
[20] Kim JR, Horton NC, Mathew SO and Mathew PA. CS1 (SLAMF7) inhibits production of proinflammatory cytokines by activated monocytes. Inflamm Res 2013; 62: 765-772.
[21] Fouquet G, Marcq I, Debuysscher V, Bayry J, Rabbind Singh A, Bengrine A, Nguyen-Khac E, Naassila M and Bouhlal H. Signaling lymphocytic activation molecules Slam and cancers: friends or foes? Oncotarget 2018; 9: 16248-16262.
[22] Raedler LA. Empliciti (Elotuzumab): first SLAMF7 antibody therapy approved for the treatment of patients with previously treated multiple myeloma. Am Health Drug Benefits 2016; 9: 74-77.
[23] Fancher KM and Bunk EJ. Elotuzumab: the first monoclonal antibody for the treatment of multiple myeloma. J Adv Pract Oncol 2016; 7: 542-547.
[24] Balasa B, Yun R, Belmar NA, Fox M, Chao DT, Robbins MD, Starling GC and Rice AG. Elotuzumab enhances natural killer cell activation and myeloma cell killing through interleukin-2 and TNF-alpha pathways. Cancer Immunol Immunother 2015; 64: 61-73.
[25] Collins SM, Bakan CE, Swartzel GD, Hofmeister CC, Efebera YA, Kwon H, Starling GC, Ciarlariello D, Bhaskar S, Briercheck EL, Hughes T, Yu J, Rice A and Benson DM Jr. Elotuzumab directly enhances NK cell cytotoxicity against myeloma via CS1 ligation: evidence for augmented NK cell function complementing ADCC. Cancer Immunol Immunother 2013; 62: 1841-1849.
[26] Lamb YN. Elotuzumab: a review in relapsed and/or refractory multiple myeloma. Drugs 2018; 78: 1481-1488.
[27] Liu YC, Szmania S and van Rhee F. Profile of elotuzumab and its potential in the treatment of multiple myeloma. Blood Lymphat Cancer 2014; 2014: 15-27.
[28] Ishibashi M, Soeda S, Sasaki M, Handa H, Imai Y, Tanaka N, Tanosaki S, Ito S, Odajima T, Sugimori H, Asayama T, Sunakawa M, Kaito Y, Kinoshita R, Kuribayashi Y, Onodera A, Moriya K, Tanaka J, Tsukune Y, Komatsu N, Inokuchi K and Tamura H. Clinical impact of serum soluble SLAMF7 in multiple myeloma. Oncotarget 2018; 9: 34784-34793.
[29] Singh DD and Yadav DK. TNBC: potential targeting of multiple receptors for a therapeutic breakthrough, nanomedicine, and immunotherapy. Biomedicines 2021; 9: 876.
[30] Latif F, Bint Abdul Jabbar H, Malik H, Sadaf H, Sarfraz A, Sarfraz Z and Cherrez-Ojeda I. Atezolizumab and pembrolizumab in triple-nega-

tive breast cancer: a meta-analysis. Expert Rev Anticancer Ther 2022; 22: 229-235.
[31] Ou-Yang F, Li CL, Chen CC, Shen YC, Moi SH, Luo CW, Xia WY, Wang YN, Lee HH, Wang LH, Wang SC, Pan MR, Hou MF and Hung MC. Deglycosylated membrane PD-L1 in tumor tissues as a biomarker for responsiveness to atezolizumab (Tecentriq) in advanced breast cancer patients. Am J Cancer Res 2022; 12: 123-137.
[32] Li CW, Lim SO, Xia W, Lee HH, Chan LC, Kuo CW, Khoo KH, Chang SS, Cha JH, Kim T, Hsu JL, Wu Y, Hsu JM, Yamaguchi H, Ding Q, Wang Y, Yao J, Lee CC, Wu HJ, Sahin AA, Allison JP, Yu D, Hortobagyi GN and Hung MC. Glycosylation and stabilization of programmed death ligand-1 suppresses T-cell activity. Nat Commun 2016; 7: 12632.
[33] Wolf MF, Ludwig A, Fritz P and Schumacher K. Increased expression of Thomsen-Friedenreich antigens during tumor progression in breast cancer patients. Tumour Biol 1988; 9: 190-194.
[34] Josic D, Martinovic T and Pavelic K. Glycosylation and metastases. Electrophoresis 2019; 40: 140-150.
[35] Munkley J and Elliott DJ. Hallmarks of glycosylation in cancer. Oncotarget 2016; 7: 35478-35489.
[36] Scott DA and Drake RR. Glycosylation and its implications in breast cancer. Expert Rev Proteomics 2019; 16: 665-680.
[37] Galili U. Amplifying immunogenicity of prospective Covid-19 vaccines by glycoengineering the coronavirus glycan-shield to present α-gal epitopes. Vaccine 2020; 38: 6487-6499.
[38] Grant OC, Montgomery D, Ito K and Woods RJ. Analysis of the SARS-CoV-2 spike protein glycan shield reveals implications for immune recognition. Sci Rep 2020; 10: 14991.
[39] Greco B, Malacarne V, De Girardi F, Scotti GM, Manfredi F, Angelino E, Sirini C, Camisa B, Falcone L, Moresco MA, Paolella K, Di Bono M, Norata R, Sanvito F, Arcangeli S, Doglioni C, Ciceri F, Bonini C, Graziani A, Bondanza A and Casucci M. Disrupting N-glycan expression on tumor cells boosts chimeric antigen receptor T cell efficacy against solid malignancies. Sci Transl Med 2022; 14: eabg3072.
[40] Lee HH, Wang YN, Xia W, Chen CH, Rau KM, Ye L, Wei Y, Chou CK, Wang SC, Yan M, Tu CY, Hsia TC, Chiang SF, Chao KSC, Wistuba II, Hsu JL, Hortobagyi GN and Hung MC. Removal of N-linked glycosylation enhances PD-L1 detection and predicts anti-PD-1/PD-L1 therapeutic efficacy. Cancer Cell 2019; 36: 168-178, e164.
[41] Breitling J and Aebi M. N-linked protein glycosylation in the endoplasmic reticulum. Cold Spring Harb Perspect Biol 2013; 5: a013359.
[42] Ruan Z, Liang M, Lai M, Shang L, Deng X and Su X. KYA1797K down-regulates PD-L1 in colon cancer stem cells to block immune evasion by suppressing the beta-catenin/STT3 signaling pathway. Int Immunopharmacol 2020; 78: 106003.
[43] Hsu JM, Xia W, Hsu YH, Chan LC, Yu WH, Cha JH, Chen CT, Liao HW, Kuo CW, Khoo KH, Hsu JL, Li CW, Lim SO, Chang SS, Chen YC, Ren GX and Hung MC. STT3-dependent PD-L1 accumulation on cancer stem cells promotes immune evasion. Nat Commun 2018; 9: 1908.
[44] Huang HC, Lai YJ, Liao CC, Yang WF, Huang KB, Lee IJ, Chou WC, Wang SH, Wang LH, Hsu JM, Sun CP, Kuo CT, Wang J, Hsiao TC, Yang PJ, Lee TA, Huang W, Li FA, Shen CY, Lin YL, Tao MH and Li CW. Targeting conserved N-glycosylation blocks SARS-CoV-2 variant infection in vitro. EBioMedicine 2021; 74: 103712.
[45] Huang HC, Liao CC, Wang SH, Lee IJ, Lee TA, Hsu JM, Kuo CT, Wang J, Hsieh WC, Chang SJ, Chen SY, Tao MH, Lin YL, Lai YJ and Li CW. Hyperglycosylated spike of SARS-CoV-2 gamma variant induces breast cancer metastasis. Am J Cancer Res 2021; 11: 4994-5005.
[46] Zhang X, Huang AC, Chen F, Chen H, Li L, Kong N, Luo W and Fang J. Novel development strategies and challenges for anti-Her2 antibody-drug conjugates. Antib Ther 2022; 5: 18-29.
[47] Schwarz F and Aebi M. Mechanisms and principles of N-linked protein glycosylation. Curr Opin Struct Biol 2011; 21: 576-582.
[48] Ruiz-Canada C, Kelleher DJ and Gilmore R. Cotranslational and posttranslational N-glycosylation of polypeptides by distinct mammalian OST isoforms. Cell 2009; 136: 272-283.
[49] Esko JD, Kimata K and Lindahl U. Proteoglycans and Sulfated Glycosaminoglycans. In: Varki A, Cummings RD, Esko JD, Freeze HH, Stanley P, Bertozzi CR, Hart GW, Etzler ME, editors. Essentials of Glycobiology. Cold Spring Harbor (NY): Cold Spring Harbor Laboratory Press Copyright © 2009, The Consortium of Glycobiology Editors, La Jolla, California.; 2009. p.
[50] Chen J, Zhong MC, Guo H, Davidson D, Mishel S, Lu Y, Rhee I, Pérez-Quintero LA, Zhang S, Cruz-Munoz ME, Wu N, Vinh DC, Sinha M, Calderon V, Lowell CA, Danska JS and Veillette A. SLAMF7 is critical for phagocytosis of haematopoietic tumour cells via Mac-1 integrin. Nature 2017; 544: 493-497.
[51] Li D, Xiong W, Wang Y, Feng J, He Y, Du J, Wang J, Yang M, Zeng H, Yang YG, Wu N, Chen S and Dong Z. SLAMF3 and SLAMF4 are immune checkpoints that constrain macrophage phagocytosis of hematopoietic tumors. Sci Immunol 2022; 7: eabj5501.

[52] He Y, Bouwstra R, Wiersma VR, de Jong M, Jan Lourens H, Fehrmann R, de Bruyn M, Ammatuna E, Huls G, van Meerten T and Bremer E. Cancer cell-expressed SLAMF7 is not required for CD47-mediated phagocytosis. Nat Commun 2019; 10: 533.

[53] Li CW, Lim SO, Chung EM, Kim YS, Park AH, Yao J, Cha JH, Xia W, Chan LC, Kim T, Chang SS, Lee HH, Chou CK, Liu YL, Yeh HC, Perillo EP, Dunn AK, Kuo CW, Khoo KH, Hsu JL, Wu Y, Hsu JM, Yamaguchi H, Huang TH, Sahin AA, Hortobagyi GN, Yoo SS and Hung MC. Eradication of triple-negative breast cancer cells by targeting glycosylated PD-L1. Cancer Cell 2018; 33: 187-201, e110.

[54] DeAngelo DJ, Jonas BA, Liesveld J, O'Dwyer M, Bixby D, Advani AS, Marlton P, Magnani J, Thackray HM and Becker PS. GMI-1271, a novel E-selectin antagonist, in combination with chemotherapy in relapsed/refractory AML. J Clin Oncol 2017; 35: 2520-2520.

[55] Ye J, Ma N, Madden TL and Ostell JM. IgBLAST: an immunoglobulin variable domain sequence analysis tool. Nucleic Acids Res 2013; 41: W34-40.

[56] Li Q, Guan X, Wu P, Wang X, Zhou L, Tong Y, Ren R, Leung KSM, Lau EHY, Wong JY, Xing X, Xiang N, Wu Y, Li C, Chen Q, Li D, Liu T, Zhao J, Liu M, Tu W, Chen C, Jin L, Yang R, Wang Q, Zhou S, Wang R, Liu H, Luo Y, Liu Y, Shao G, Li H, Tao Z, Yang Y, Deng Z, Liu B, Ma Z, Zhang Y, Shi G, Lam TTY, Wu JT, Gao GF, Cowling BJ, Yang B, Leung GM and Feng Z. Early transmission dynamics in Wuhan, China, of novel coronavirus-infected pneumonia. N Engl J Med 2020; 382: 1199-1207.

[57] Rajasekharan S, Milan Bonotto R, Nascimento Alves L, Kazungu Y, Poggianella M, Martinez-Orellana P, Skoko N, Polez S and Marcello A. Inhibitors of protein glycosylation are active against the coronavirus severe acute respiratory syndrome coronavirus SARS-CoV-2. Viruses 2021; 13: 808.

[58] Yu C, Li S, Zhang X, Khan I, Ahmad I, Zhou Y, Li S, Shi J, Wang Y and Zheng YH. MARCH8 inhibits ebola virus glycoprotein, human immunodeficiency virus type 1 envelope glycoprotein, and avian influenza virus H5N1 hemagglutinin maturation. mBio 2020; 11: e01882-20.

[59] Shrivastava-Ranjan P, Bergeron E, Chakrabarti AK, Albarino CG, Flint M, Nichol ST and Spiropoulou CF. 25-hydroxycholesterol inhibition of lassa virus infection through aberrant GP1 glycosylation. mBio 2016; 7: e01808-16.

[60] Lopez-Sambrooks C, Shrimal S, Khodier C, Flaherty DP, Rinis N, Charest JC, Gao N, Zhao P, Wells L, Lewis TA, Lehrman MA, Gilmore R, Golden JE and Contessa JN. Oligosaccharyltransferase inhibition induces senescence in RTK-driven tumor cells. Nat Chem Biol 2016; 12: 1023-1030.

[61] Lum LG, Thakur A, Elhakiem A, Alameer L, Dinning E and Huang M. Anti-CS1 × Anti-CD3 bispecific antibody (BiAb)-armed anti-CD3 activated T cells (CS1-BATs) kill CS1(+) myeloma cells and release type-1 cytokines. Front Oncol 2020; 10: 544.

[62] Gogishvili T, Danhof S, Prommersberger S, Rydzek J, Schreder M, Brede C, Einsele H and Hudecek M. SLAMF7-CAR T cells eliminate myeloma and confer selective fratricide of SLAMF7(+) normal lymphocytes. Blood 2017; 130: 2838-2847.

[63] Bhutani D and Lum LG. Activated T cells armed with bispecific antibodies kill tumor targets. Curr Opin Hematol 2015; 22: 476-483.

[64] Vij R, Nath R, Afar DEH, Mateos MV, Berdeja JG, Raab MS, Guenther A, Martínez-López J, Jakubowiak AJ, Leleu X, Weisel K, Wong S, Gulbranson S, Sheridan JP, Reddy A, Paiva B, Singhal A, San-Miguel JF and Moreau P. First-in-human phase I study of ABBV-838, an antibody-drug conjugate targeting SLAMF7/CS1 in patients with relapsed and refractory multiple myeloma. Clin Cancer Res 2020; 26: 2308-2317.

[65] Cho SF, Xing L, Anderson KC and Tai YT. Promising antigens for the new frontier of targeted immunotherapy in multiple myeloma. Cancers (Basel) 2021; 13: 6136.

[66] Li CW, Xia W, Huo L, Lim SO, Wu Y, Hsu JL, Chao CH, Yamaguchi H, Yang NK, Ding Q, Wang Y, Lai YJ, LaBaff AM, Wu TJ, Lin BR, Yang MH, Hortobagyi GN and Hung MC. Epithelial-mesenchymal transition induced by TNF-α requires NF-κB-mediated transcriptional upregulation of Twist1. Cancer Res 2012; 72: 1290-1300.

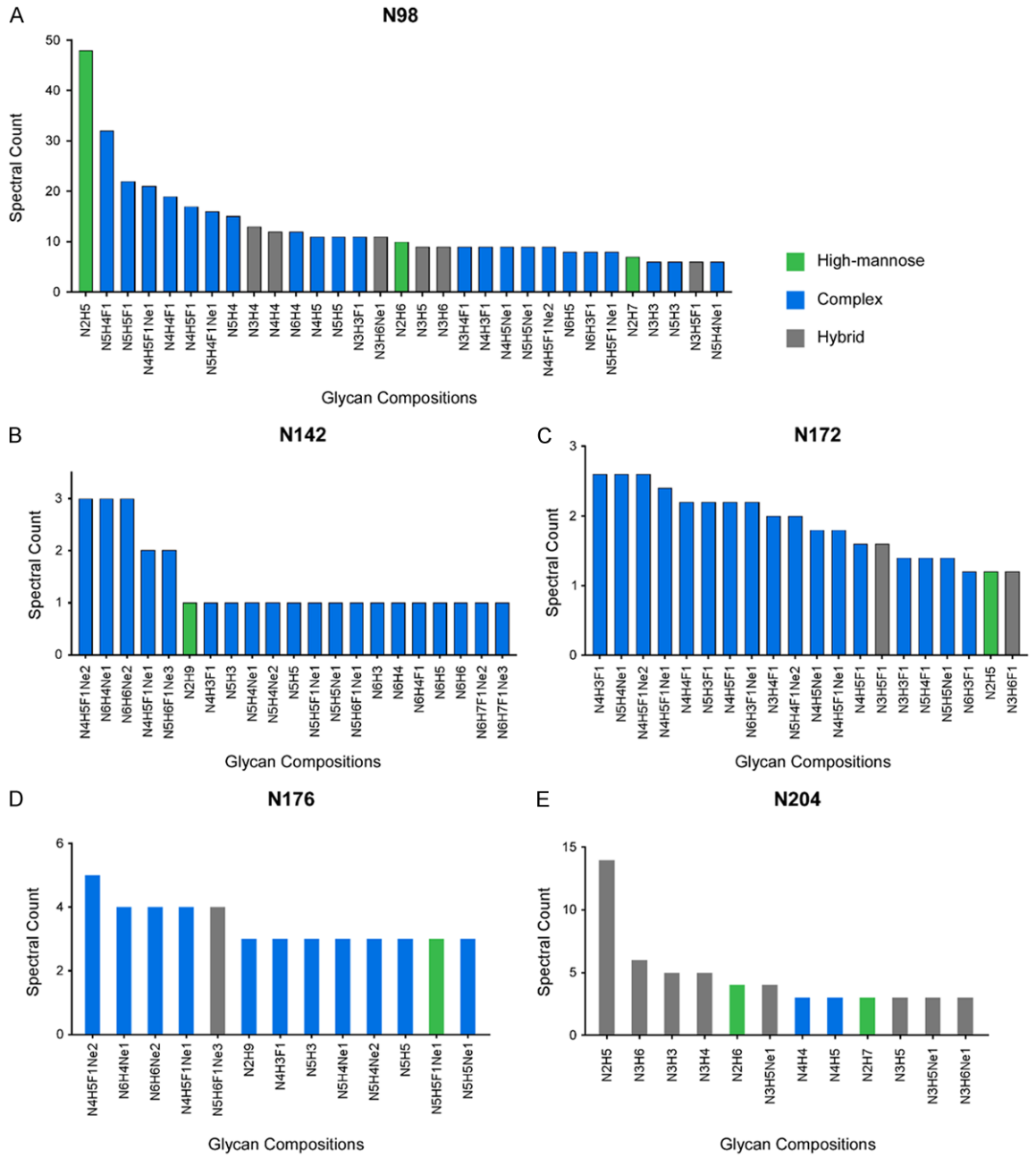

Figure S1. Glycan composition of N-link glycosylation sites at (A) N98, (B) N142, (C) N172, (D) N176, and (E) N204 of SLAMF7.

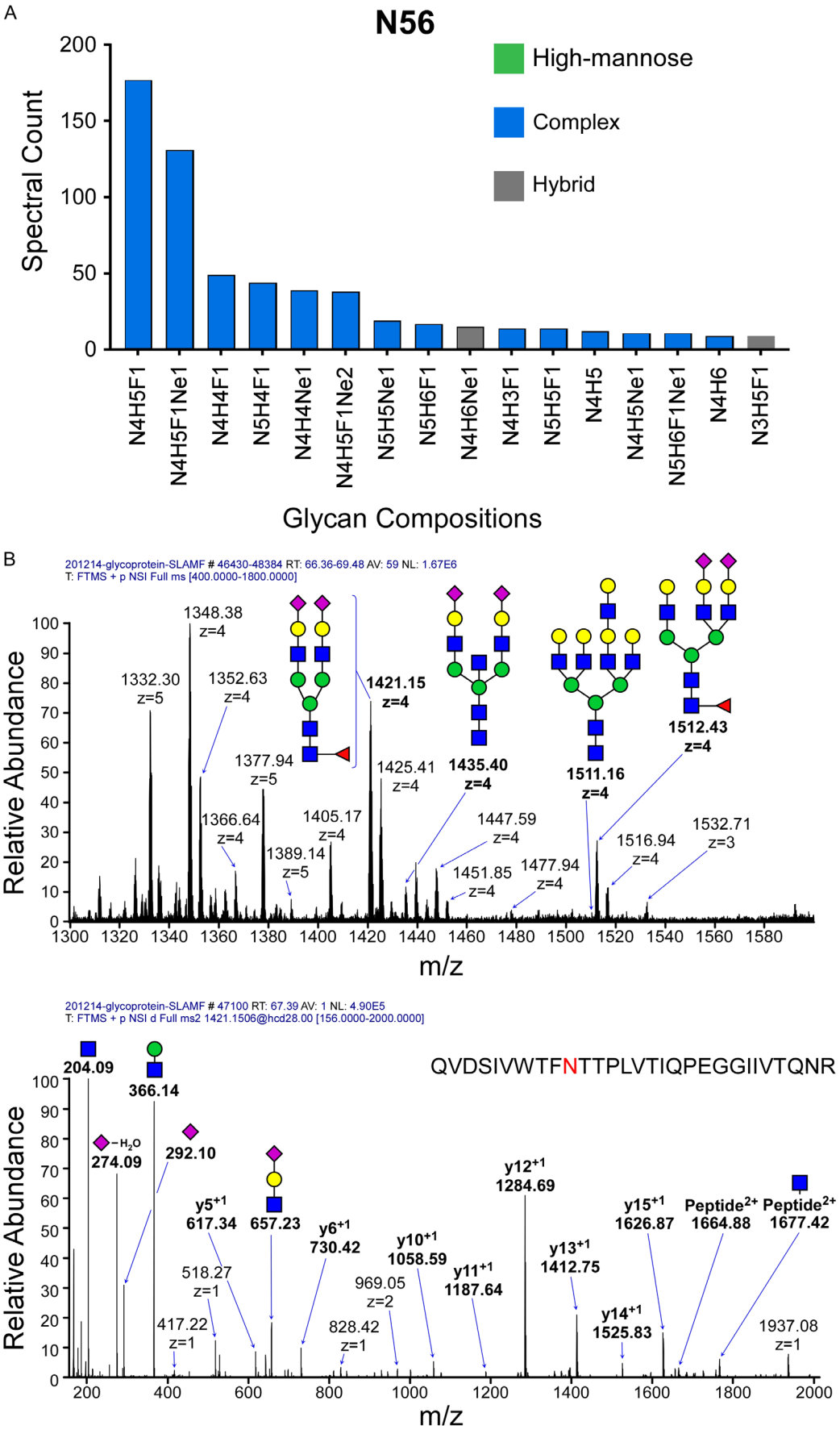
A
N56
High-mannose
Complex
Hybrid
Spectral Count
200
150
100
50
0
N4H5F1
N4H5F1Ne1
N4H4F1
N5H4F1
N4H4Ne1
N4H5F1Ne2
N5H5Ne1
N5H6F1
N4H6Ne1
N4H3F1
N5H5F1
N4H5
N4H5Ne1
N5H6F1Ne1
N4H6
N3H5F1
Glycan Compositions
B
201214-glycoprotein-SLAMF # 46430-48384 RT: 66.36-69.48 AV: 59 NL: 1.67E6
T: FTMS + p NSI Full ms [400.0000-1800.0000]
Relative Abundance
m/z
1348.38 z=4
1332.30 z=5
1352.63 z=4
1421.15 z=4
1377.94 z=5
1425.41 z=4
1435.40 z=4
1511.16 z=4
1512.43 z=4
1366.64 z=4
1405.17 z=4
1389.14 z=5
1447.59 z=4
1451.85 z=4
1477.94 z=4
1516.94 z=4
1532.71 z=3
201214-glycoprotein-SLAMF # 47100 RT: 67.39 AV: 1 NL: 4.90E5
T: FTMS + p NSI d Full ms2 1421.1506@hcd28.00 [156.0000-2000.0000]
QVDSIVWTFNTTPLVTIQPEGGIIVTQNR
Relative Abundance
m/z
204.09
366.14
−H2O 274.09
292.10
y5+1 617.34
657.23
y6+1 730.42
518.27 z=1
417.22 z=1
828.42 z=1
969.05 z=2
y10+1 1058.59
y11+1 1187.64
y12+1 1284.69
y13+1 1412.75
y14+1 1525.83
y15+1 1626.87
Peptide2+ 1664.88
Peptide2+ 1677.42
1937.08 z=1

Figure S2. N56 of SLAMF7 is heavily glycosylated. A. Glycan composition of N-link glycosylation sites at N56 of SLAMF7. B. LC-MS/MS-based identification of N56 glycopeptides. The LC-MS profiles are shown as spectra averaged throughout elution time when a representative subset of glycoforms was detected. The cartoon symbols used for the glycans conform to the standard representation recommended by the Consortium for Functional Glycomics.

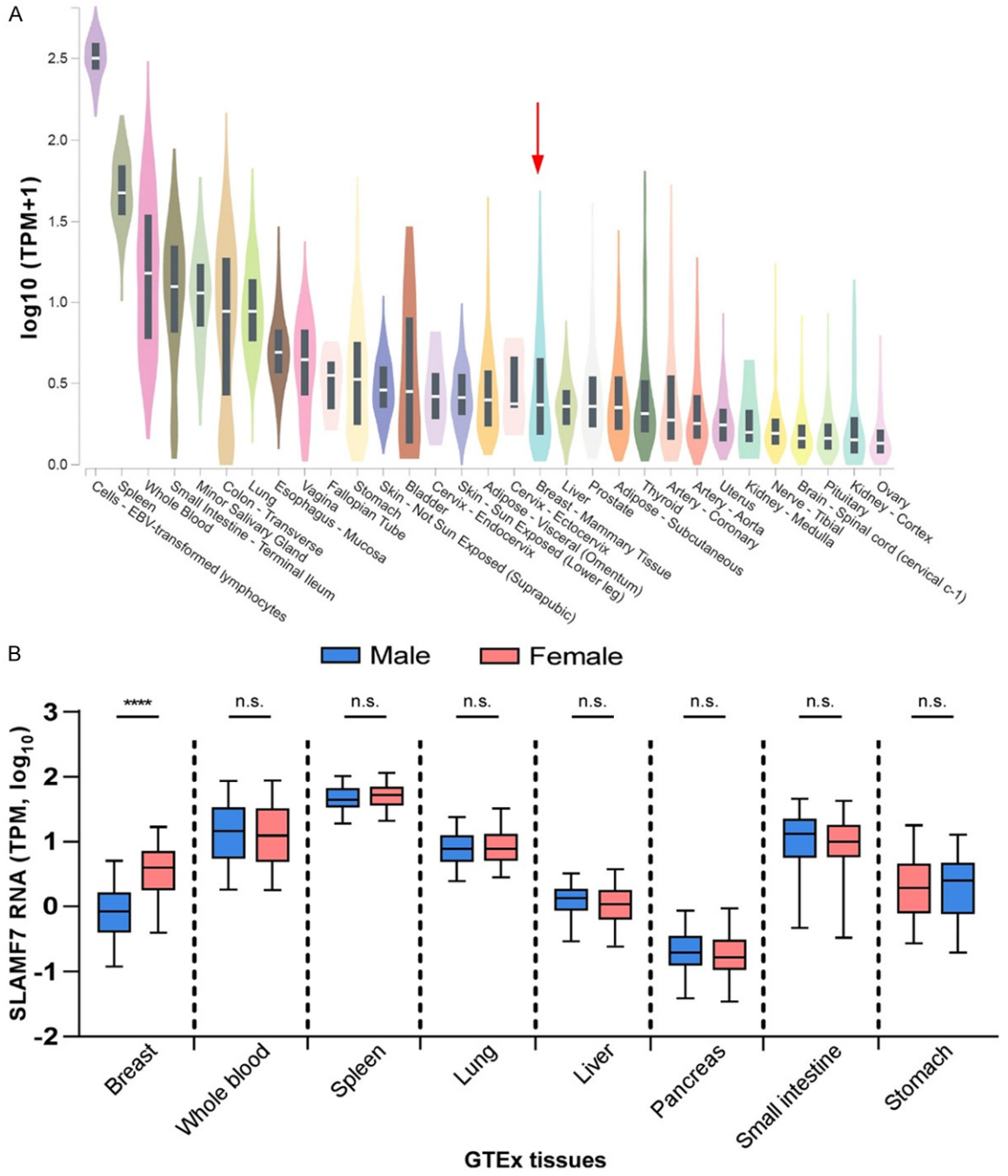

Figure S3. SLAMF7 RNA expression in normal tissue. A. RNA expression profile of SLAMF7 in normal tissue-derived GTEx dataset. B. Comparison of SLAMF7 expression between the male and female group in normal tissue-derived GTEx dataset. ****, $P<0.0001$. *P*-values were calculated by *t*-test.